Non-pathogenic leaf-colonising bacteria elicit pathogen-like responses in a colonisation density-dependent manner

Moritz Miebach[1,2], Léa Faivre[3], Daniel Schubert[3], Paula Jameson[1], Mitja Remus-Emsermann[1,2,3]

[1] School of Biological Sciences, University of Canterbury, Christchurch 8140, New Zealand
[2] Biomolecular Interaction Centre, University of Canterbury, Christchurch 8140, New Zealand
[3] Institute of Microbiology and Dahlem Centre of Plant Sciences, Department of Biology, Chemistry, Pharmacy, Freie Universität Berlin, Berlin 14195, Germany

Plain Language Summary

Plants are colonised by diverse bacteria affecting many aspects of plant life. Here we show that plants do not differentiate between different bacteria but measure their quantities to keep bacterial numbers in check.

Abstract

Leaves are colonised by a complex mix of microbes, termed the leaf microbiota. Even though the leaf microbiota is increasingly recognised as an integral part of plant life and health, our understanding of its interactions with the plant host is still limited. Here, mature, axenically grown *Arabidopsis thaliana* plants were spray-inoculated with six diverse leaf-colonising bacteria. The transcriptomic changes in leaves were tracked over time and significant changes in ethylene marker (*ARL2*) expression were observed only two to four days after spray-inoculation. Whole transcriptome sequencing revealed that four days after inoculation, leaf transcriptional changes to colonisation by non-pathogenic and pathogenic bacteria differed in strength but not in the type of response. Inoculation of plants with different densities of the non-pathogenic bacterium *Williamsia* sp. Leaf354 showed that high bacterial titers caused disease phenotypes and led to severe transcriptional reprogramming with a strong focus on plant defence. An *in silico*

31 epigenetic analysis of the data was congruent with the transcriptomic analysis. These
32 findings suggest (1) that plant responses are not rapid after spray-inoculation, (2) that plant
33 responses only differ in strength and (3) that plants respond to high titers of non-
34 pathogenic bacteria with pathogen-like responses.
35

36 ## Introduction

37

38 Plants are colonised by a vast variety of bacteria with various effects on plant health and
39 growth, ranging from pathogens to nitrogen-fixing rhizobacteria (Wang *et al.*, 2018; Kelly *et*
40 *al.*, 2018). Past research mainly focused on a few important microbiota members,
41 overlooking most of the remarkably diverse microbes present on and within plants.
42 Increasing evidence showcases the positive effects of the plant microbiota on its host,
43 including the protection against abiotic (Lau & Lennon, 2012) and biotic (Innerebner *et al.*,
44 2011; Ritpitakphong *et al.*, 2016; Zengerer *et al.*, 2018; Vogel *et al.*, 2021) stressors, the
45 promotion of growth (Spaepen *et al.*, 2009) and the assimilation of specific nutrients
46 (Hacquard *et al.*, 2015; Singh *et al.*, 2022). Some of these beneficial effects are solely
47 attributed to microbes, whereas others involve the plant as an interaction partner. For
48 example, with regard to the protection against biotic stress, some microbes can protect the
49 plant from a pathogen via resource competition with the pathogen (Ji & Wilson, 2002) or
50 the production of antimicrobials targeting the pathogen (Zengerer *et al.*, 2018), whereas
51 others stimulate the plant immune system, leading to increased immune responses upon
52 subsequent infection with a pathogen (Pieterse *et al.*, 1996; Vogel *et al.*, 2016, 2021).
53

54 Even though the microbiota seems to be an integral part of plant life, our understanding of
55 its interaction with the host is still limited. Studies on plant pathogens have shown that
56 early perception of microbes is conferred by the detection of microbe-associated molecular
57 patterns (MAMPs). MAMPs are conserved traits of microbes irrespective of their symbiotic
58 relationship with the plant, raising the question if and how plants discriminate between
59 pathogenic and beneficial bacteria. Recently, it was shown that plants respond to diverse
60 non-pathogenic leaf colonisers, at varying intensities of transcriptional reprogramming

(Maier *et al.*, 2021). However, whether the amount of transcriptional reprogramming is caused by the different identities of the bacteria is unclear. Notably, the observed plant response was enriched for plant defence-associated genes and measured nine days after inoculation of ten-days-old seedlings, indicating persistently active immune responses. This is intriguing, since plant immune responses infer a growth penalty, commonly referred to as the growth-defence tradeoff (Huot *et al.*, 2014; He *et al.*, 2022).

As a persistent immune activation infers a growth penalty, plants need to activate their immune system according to potential pathogen threat in a timely manner (Huot *et al.*, 2014; He *et al.*, 2022). Different activation kinetics likely lead to different downstream signalling events and finally to a different immune response, highlighting the importance of time-resolved analyses. In other words, MAMPs are present early in the plant-microbe interaction and lead to early plant responses. However, MAMPs are less indicative of the symbiotic relationship between the microbe and the plant compared to effector proteins. Accordingly, plant responses triggered by MAMPs are more transient than those triggered by effector molecules (Gao et al., 2013; Lamb & Dixon, 1997; Tsuda et al., 2013). Plant responses to different MAMPs are almost identical early after MAMP application, but differ later, resulting in differential immune outputs (Zipfel *et al.*, 2006; Kim *et al.*, 2014; Bjornson *et al.*, 2021). Elf18 and chitosan, for example, predominantly activate jasmonic acid (JA)-mediated immune responses early on, resulting in JA-mediated immunity later, while flg22 activates jasmonic acid (JA)-mediated and ethylene (ET)-mediated immune responses early on, resulting in salicylic acid (SA)-mediated immunity later (Kim *et al.*, 2014). This further highlights the importance of time-resolved analyses and suggests that, already at the level of MAMP recognition, plant immune responses differ depending on the cocktail of MAMPs present.

The response of plants to leaf colonisation, whether by pathogenic or non-pathogenic bacteria, involves a significant transcriptome reprogramming (Moore *et al.*, 2011; Maier *et al.*, 2021). This reprogramming relies on the interaction of numerous transcription factors with the local chromatin environment. Indeed, several histone modifications such as

91 H3K4me3, H3K36me3 and lysine acetylation were found to contribute to the induction of
92 genes following pathogen exposure (Berr *et al.*, 2012; Ding & Wang, 2015). By contrast,
93 transcriptional reprogramming following colonisation by non-pathogenic bacteria has not
94 been investigated.
95
96 To monitor the dynamics of plant immune responses, we inoculated plants with diverse
97 bacteria, including a plant pathogen, and measured transcriptional outputs, representing the
98 three major phytohormone pathways in plant immunity (SA, JA and ET), at various times
99 after inoculation. As the strongest responses were observed 96 hours post inoculation (hpi),
100 we measured the whole transcriptional plant responses at this time. Interestingly, plant
101 responses to various bacterial inoculants strongly overlapped and we observed a trend that
102 the plant responses were dependent on bacterial density. Most differentially expressed
103 genes in response to one isolate were also differentially expressed in response to isolates
104 that exhibited overall stronger responses. The question then arose whether non-pathogenic
105 bacteria could induce plant defence responses at artificially high colonisation densities. To
106 address this question, we assessed the effects of different bacterial densities of the non-
107 pathogenic leaf coloniser *Williamsia* sp. Leaf354 on *in planta* transcription as well as on
108 plant health and plant weight 96 hpi and 21 dpi, respectively, to test the hypothesis that
109 plants are monitoring bacterial population density rather than differentiating between
110 different bacterial colonisers. Finally, in an effort to uncover chromatin marks that might
111 contribute to transcriptional responses to non-pathogenic leaf colonisers, we performed an
112 *in silico* chromatin analysis.
113

Materials and Methods

Plant growth: Plants were grown as previously described in (Miebach *et al.*, 2020). Briefly, sterilised seeds were germinated on ½ MS (Murashige and Skoog medium, including vitamins, Duchefa, Haarlem, Netherlands) 1% phytoagar (Duchefa) filled pipette tips. Healthy looking seedlings were aseptically transferred, without removal from the pipette tip, aseptically into Magenta boxes (Magenta vessel GA-7, Magenta LLC, Lockport, IL, USA) filled with ground Zeolite (sourced from cat litter - Vitapet, Purrfit Clay Litter, Masterpet New Zealand, Lower Hutt, New Zealand) and watered with 60 mL ½ MS. Each box received four seedlings. The boxes were closed with lids that allowed for gas exchange and placed into a climate cabinet (85% relative humidity, 11 h light, 13 dark, 21 °C, 150-200 µmol light intensity). Plants were grown for four weeks for the time course and six weeks for the bacterial density experiment before they were treated with bacteria or mock controls.

Plant inoculation: Bacterial suspensions were prepared as previously described in (Miebach *et al.*, 2020). Briefly, bacteria were cultivated at 30 °C on minimal media agar plates containing 0.1% pyruvate as a carbon source. Bacterial suspensions were prepared from bacterial colonies suspended in phosphate-buffered saline (PBS, 0.2 g L^{-1} NaCl, 1.44 g L^{-1} Na_2HPO_4 and 0.24 g L^{-1} KH_2PO_4) and washed twice via centrifugation at 4000 × *g* for 5 min followed by discarding the supernatant and again adding PBS. Table **1** contains the list of bacteria used in this study. For the time course experiment the optical density ($OD_{600\ nm}$) was adjusted so that the suspension contained 2×10^7 colony forming units (CFU) ml^{-1}. To explore the influence of bacterial load on plant responses, the bacterial suspensions were adjusted to 10^5, 10^6, 10^7 and 10^8 CFU ml^{-1}. Next, 200 µL (time course experiment) or 1 ml (bacterial load experiment) of bacterial solution was sprayed per plant tissue culture box using an airbrush spray gun (0.2 mm nozzle diameter, Pro Dual Action 3 #83406). To obtain a homogeneous coverage, the distance between the airbrush spray gun and the plants was increased by stacking a plant tissue culture box, with the bottom cut off, onto the plant tissue culture box containing the plants being spray-inoculated.

143 **Table 1: List of bacterial strains used in this study.**

Bacterial Strain	Reference	Abbreviation
Pseudomonas syringae DC3000	(Cuppels, 1986)	Pst
Sphingomonas sp. Leaf34	(Bai *et al.*, 2015)	Sphingo34
Acidovorax sp. Leaf84	(Bai *et al.*, 2015)	Acido84
Microbacterium sp. Leaf347	(Bai *et al.*, 2015)	Micro347
Williamsia sp. Leaf354	(Bai *et al.*, 2015)	Willi354
Pedobacter sp. Leaf194	(Bai *et al.*, 2015)	Pedo194

144

145 *Bacterial enumeration:* Above ground plant parts were detached from belowground parts
146 using sterilised equipment and placed individually into pre-weighed 1.5 mL tubes. After
147 determining the plant weight 1 mL PBS 0.02% Silwet L-77 (Helena Chemical Company) was
148 added to each tube. Bacteria were dislodged from the sample by shaking twice at 2.6 m s^{-1}
149 for 5 min (Omni Bead Ruptor 24) and sonication for 5 min. Bacterial CFU were enumerated
150 using plate counting on R2A media plates.
151
152 *Gene expression analysis:* Four-weeks-old and six-weeks-old plants were spray-
153 inoculated with individual strains (Table **1**) or PBS (mock control) for the time course and
154 bacterial load experiment, respectively. For the time course experiment above ground
155 plant parts were harvested after 1, 3, 6, 9, 12, 24, 48, and 96 h post inoculation (hpi). For the
156 bacterial load experiment above ground plant parts were harvested 96 hpi. The plant
157 material was collected in RNase-free microcentrifuge tubes (MCT-150-C, Axygen, Corning,
158 USA) and was then immediately flash frozen in liquid N_2. Two plants from different
159 growth boxes were pooled per tube to form a biological replicate. Three biological
160 replicates were sampled per treatment and time point. Flash-frozen samples were ground

161 to a fine powder in the collection tube using Teflon pestles (General Lab Supply, Lab
162 Supply, Dunedin, New Zealand). RNA extraction was performed using the Isolate II RNA
163 Plant kit (Bioline, London, England).

164

165 *RT-qPCR analysis:* For cDNA synthesis, 1 µg of RNA was used and for the no Reverse
166 Transcriptase (noRT) control, using the VitaScript First strand cDNA synthesis kit
167 (Procomcure Biotech, Thalgau, Austria). RT-qPCR was performed using the 2× ProPlant
168 SYBR Mix (Procomcure Biotech) in 15 µL reaction volumes with 0.2 µM of each primer and
169 0.001 g L^{-1} of initial RNA in the cDNA mix. QPCRs were run using the recommended
170 protocol for 2× ProPlant SYBR Mix (Procomcure Biotech) on a Rotor-Gene Q (Qiagen,
171 Hilden, Germany). Technical triplicates were performed for each sample. The ROX dye,
172 present in the 2× ProPlant SYBR Mix, was used to normalise for master mix variation
173 between tubes. A mix of equal amounts of all cDNAs was used for normalisation between
174 runs. mRNA concentrations were calculated using Equation (1).

175 (1) $mRNA\ concentration\ (a.u.) = 1/(primer\ efficiency)^{Cq}$

176

177 Primers that were first used in this study were designed using 'primer-blast' (NCBI,
178 Bethesda, MD, USA). Primer efficiencies were determined via serial template dilutions
179 (Nolan *et al.*, 2013). The mRNA concentration of each target gene was then normalised
180 against the mean mRNA concentration of two stably expressed, previously described
181 reference genes (Table **2**, (Czechowski *et al.*, 2005)). Next, the normalised mRNA
182 concentration of each treatment (bacterial inoculation) was normalised against the mean
183 normalised mRNA concentration of mock-treated samples to emphasise treatment-related
184 changes in gene expression (Denoux *et al.*, 2008).

185 **Table 2: List of primers used in this study.**

Template	Reference	5` primer (forward)	3` primer (reverse)
ARL2	(Miebach *et al.*, 2020)	cgaaccgtccgtacatacataa	ttgcacgaaactaaaactaaaagc
PR1	(Miebach *et al.*, 2020)	gatgtgccaaagtgaggtgtaa	ttcacataattcccacgagga
At3g50280	This work	ccttcgctggtcgtcttaac	cagagccatcaggtcgaaga
VSP1	(Dombrecht *et al.*, 2007)	ggacttgccctaaagaacga	gtgttctcggtcccatatcc
LOX2	(Vogel *et al.*, 2016)	agtcttcacgccaggctatg	gagtcctcaaccaatgggaa
ERF1	(Vogel *et al.*, 2016)	agttcaagagtcgctttcgg	tcgagtgtttcctcttcaacg
PAD3	(La Camera *et al.*, 2011)	tgctcccaagacagacaatg	gttttggatcacgacccatc
CRK5	(Vogel *et al.*, 2016)	tcaccactagacctcgtggatt	gtaagcatttggacgatcgc
CRK23	(Vogel *et al.*, 2016)	gctactccagtggattccga	aaaggcgacacagttatggc
AT1G51890	(Vogel *et al.*, 2016)	tgcttgagaccgctcattta	aagctgggaaacaagaatgc
SWEET4	(Chen *et al.*, 2010)	ccatcatgagtaaggtgatcaaga	caaaatgaaaaggtcgaacttaataagtg
SWEET12	(Chen *et al.*, 2010)	aaagctgatatctttcttactacttcgaa	cttacaaatcctatagaacgttggcac
STP13	(Yamada *et al.*, 2016)	tgtttctgtttaactccttgagaga	ttcgccgaagtcgcaaatcctcctc

At2g28390 (reference)	(Miebach *et al.*, 2020)	ggattttcagctactcttcaagcta	tcctgccttgactaagttgaca
At4g26410 (reference)	(Miebach *et al.*, 2020)	cgtccacaaagctgaatgtg	cgaagtcatggaagccactt

186

187 *RNA sequencing:* RNA library preparation and sequencing was performed by Custom
188 Science (Epping, Australia). RNA quality and purity was assessed using a Nanodrop (ND-
189 2000 Spectrophotometer, Thermo Scientific, Waltham, MA, USA). RNA integrity was
190 verified on a 2100 Bioanalyzer (Agilent, Santa Clara, CA, USA) using the RNA 6000 Nano Kit
191 (Agilent). Poly-A enriched libraries were prepared using the NEBNext UltraTM RNA Library
192 Prep Kit (New England Biolabs, Ipswich, USA) for Illumina. RNA sequencing was performed
193 on a NovaSeq 6000 (Illumina, San Diego, USA) platform. Approximately 30,000,000 paired-
194 end reads with a length of 150 bp were generated per sample. Adapters and low-quality
195 reads (end sequences with base quality < 20 and sequences with N content > 10%) were
196 removed from raw sequences and sequences below 75 bp were filtered using cutadapt
197 (v1.9.1) (Martin, 2011). The resulting reads were mapped against the *Arabidopsis thaliana*
198 (arabidopsis) reference genome (TAIR10). Mapped reads were counted with featureCounts
199 (v1.22.2) (Liao *et al.*, 2014).

200

201 *RNA sequencing data analysis:* Genes above 0.5 counts per million in at least three
202 samples were used for differential gene expression analysis using edgeR (Robinson *et al.*,
203 2010). Counts were scaled to effective library sizes by the trimmed mean of M values
204 method (Robinson & Oshlack, 2010). Gene-wise dispersions were estimated via Cox-Reid
205 profile-adjusted likelihood and squeezed to trended dispersions using an empirical Bayes
206 method (McCarthy *et al.*, 2012). Genes were determined as differentially expressed using
207 the TREAT method under edgeRs general linear model framework (McCarthy & Smyth,
208 2009). Genes with a fold change (FC) significantly above $\log_2(1.3)$ and below a False
209 Discovery Rate (FDR; Benjamini-Hochberg *p* correction) cut-off of 5% were kept as

210 differentially expressed genes (DEGs). The FC threshold was determined using elbow plots
211 (Fig. **S3a**, Fig. **S4a**). MDS plots were generated from trimmed mean of M values method
212 normalised gene counts. K-means clusters were calculated from $\log_2$-transformed counts
213 per million, that were centred around the mean for each gene. A prior count of two was
214 added to each gene count to prevent taking the logarithm of zero. Elbow plots were used to
215 determine the optimal number of Ks (Fig. **S3b**, Fig. **S4b**). Heatmaps were generated from
216 $\log_2$-transformed counts per million (cpm), that were centred around the mean for each
217 gene. GO term enrichment analysis was performed using the PANTHER classification
218 system (v17.0) (Mi *et al.*, 2021).

219 *Chromatin state analysis:* Chromatin state coordinates were obtained from (Sequeira-
220 Mendes *et al.*, 2014) and gene coordinates were obtained from the TAIR10 annotation from
221 BioMart, Plantsmart28 (Durinck *et al.*, 2005). A gene was considered to be in a certain state
222 if at least 150 bp (approximate length of DNA wrapped around one nucleosome) of its gene
223 body overlapped with the respective state. Thus, a single gene may have several distinct
224 states along its coding sequence. Genes induced or repressed after Pst exposure were
225 divided into two sets depending on whether they were also differentially expressed by
226 exposure to Micro347 or Willi354 (Non Pst-specific) or only by Pst (Pst-specific). Similarly,
227 genes induced or repressed by the highest inoculation density of Willi354 were divided
228 into two sets depending on whether they were also differentially expressed by exposure to
229 lower bacterial densities (non 10^8-specific) or not (10^8-specific). The proportion of genes of
230 interest in each chromatin state was compared with the proportion of genes in the
231 respective state in the complete genome. The significance of the difference between the
232 two proportions was tested using the Marascuilo procedure, with a confidence level of
233 0.95.

Results

The aim of this study was to broaden our knowledge of the intricate relationship between the plant and its bacterial colonisers. The focus lay on assessing plant transcriptional responses to a diverse array of microbial colonisers. Therefore, six microbial leaf colonisers representing all major phyla of the core leaf microbiota were selected (Vorholt, 2012; Bai *et al.*, 2015) (Fig. **1**).

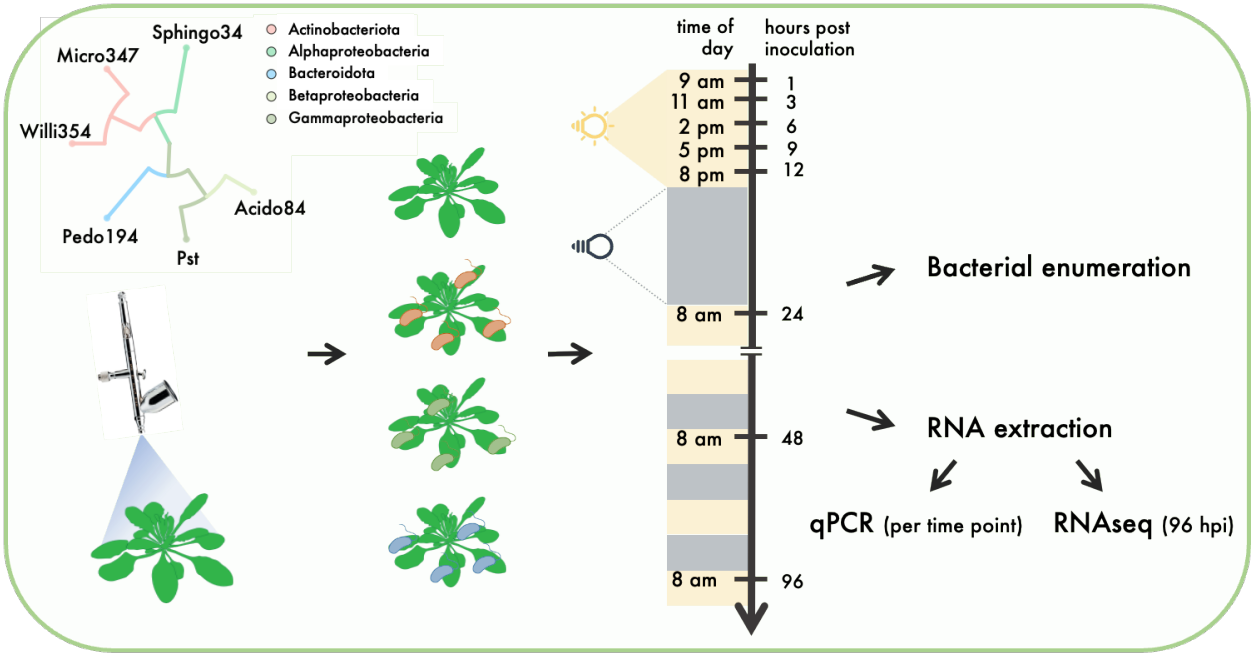

Fig. 1: Experimental design. Four-weeks-old axenically-grown *Arabidopsis thaliana* plants were spray-inoculated with individual bacterial strains, depicted in the phylogenetic tree in the top left corner of the figure. Plants were harvested at different times after inoculation. Some plants were used for bacterial enumeration and others for RNA extraction.

Temporal responses of the plant immune system

Arabidopsis plants were grown axenically in the 'Litterbox' system, to ensure (1) low artificial, but strictly controlled, growth conditions and (2) to prevent a strong inoculation of the growth media post inoculation (Miebach *et al.*, 2020). Four-weeks-old plants were spray-inoculated with individual strains of bacterial leaf colonisers, at ~ 10^5 - 10^6 bacteria per g of leaf, the bacterial carrying capacity of plants in temperate environments (Kniskern

et al., 2007; Reisberg *et al.*, 2012; Rastogi *et al.*, 2012; Burch *et al.*, 2016; Gekenidis *et al.*, 2017) . The temporal course of bacterial densities post inoculation confirmed that bacteria were sprayed close to carrying capacity. Within 4 dpi the bacterial densities for Sphingo34 and Micro347 remained stable at 10^6 bacteria per g of leaf. In contrast, the bacterial densities for Willi354 and Pst slightly rose to 10^7 bacteria per g of leaf within 4 dpi (Fig. **2a**). Interestingly, the bacterial density of Micro347 significantly ($p < 0.001$, Tukey's HSD test) dropped to ~ 10^4 bacteria per g of leaf 7 dpi. This two-magnitude drop in bacterial density cannot be explained by the increase in plant weight (Fig. **S1**) and, therefore, suggests that the bacteria were dying.

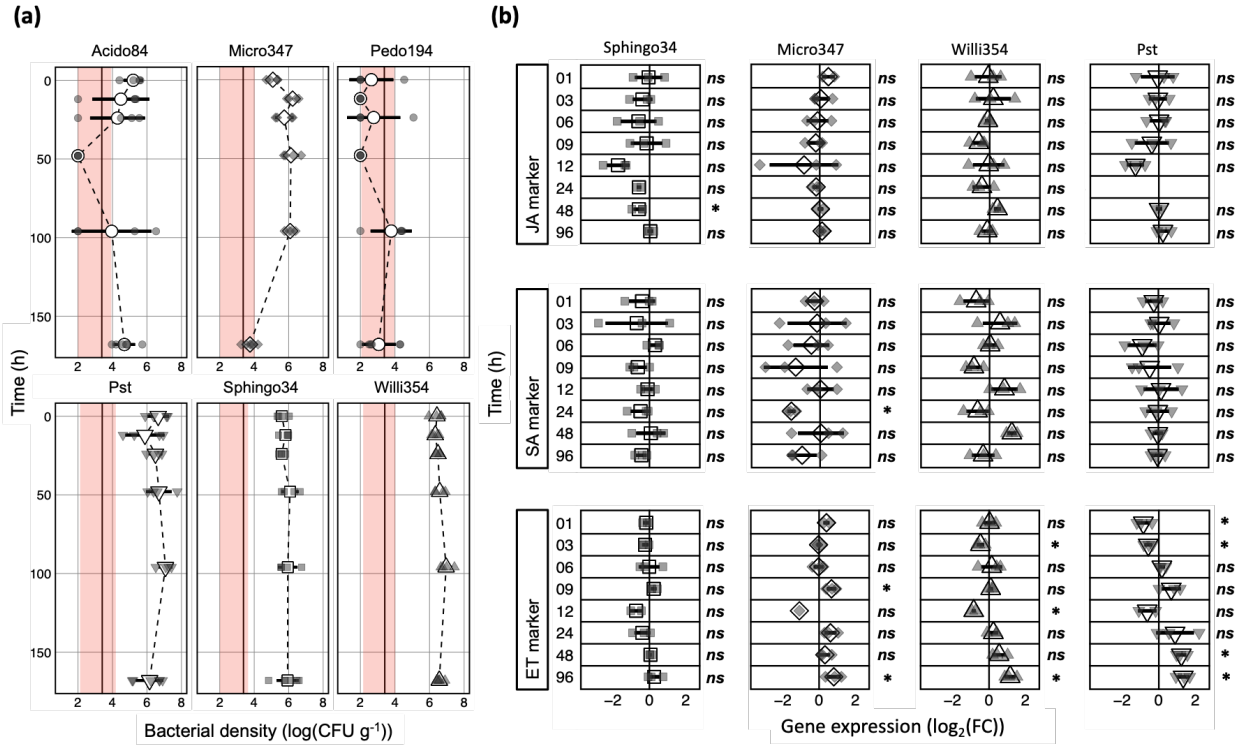

Fig. 2: Temporal transcriptional responses to bacterial colonisation. Four-weeks-old axenically-grown arabidopsis plants were spray-inoculated with individual bacterial strains (see coloured boxes; strains are sorted alphabetically in (**a**) and by response amplitude of the ethylene marker gene in (**b**)). (**a**) Bacterial density on above ground plant parts at several times post inoculation. To accommodate plants with CFU below the limit of detection, 10^2 CFU g^{-1} were added to the count of every sample. (**b**) Depicted are $\log_2$(FC) in gene expression relative to mock-treated control for a jasmonic acid (JA) marker gene (*At3g50280*), a salicylic acid (SA) marker gene (*PR1*) and an ethylene (ET) marker gene (*ARL2*). Large white shapes depict the mean, bars depict standard deviation, smaller grey shapes

271 depict individual biological replicates, dashed black line connects the means, solid black line
272 represents the lower limit of detection based on mean plant weight and the red areas represent the
273 range of the limit of detection based on the heaviest and lightest plant, * depicts statistical
274 significance (Bonferroni corrected $p < 0.05$) and *ns* depicts the lack of statistical significance, T-test.
275
276 Two out of the six bacterial leaf colonisers, Acido84 and Pedo194, failed to consistently
277 establish densities above the threshold of detection. Acido84 was recovered from some,
278 but not all plants. Whenever Acido84 was recovered it reached densities of ~ 10^5 - 10^6 CFU
279 g^{-1}. This heterogeneity in colonisation success was unlikely to have been caused by non-
280 homogeneous spray inoculation, as other inoculants exhibited considerably lower plant to
281 plant variation (Fig. **2a**). Further, all plants sampled 168 hpi harboured ~ 10^4 - 10^6 CFU g^{-1}.
282
283 Plants inoculated by one of the four successful coloniser strains, Micro347, Pst, Sphingo34
284 and Willi354, were investigated further by qPCR (Fig. **2b**). Early temporal changes in the
285 plant immune response were tracked using previously reported marker genes that follow
286 the levels of the three major phytohormones in plant immunity: ET, JA and SA (Kim *et al.*,
287 2014). Marker gene expression was measured at eight different time points ranging from 1
288 hpi to 96 hpi. As dynamic changes in expression were expected early after inoculation, five
289 of the eight measurement times fell within the first 12 hpi.
290
291 Surprisingly, gene expression changes caused by the bacterial treatments were relatively
292 weak. The strongest changes did not exceed 5-fold (maximum mean: 2.5-fold; maximum
293 individual replicate: 4.6-fold) in gene expression, relative to the mock-treated control (Fig.
294 **2b**). The strongest changes were observed in the expression of the ET marker, *ARL2*. Early
295 after inoculation, its expression dropped significantly, at 1 and 3 hpi for Pst and 3 hpi for
296 Willi354. After recovering to the expression levels found in mock-treated plants the
297 relative expression of the ET marker dropped again at 12 hpi, which was significant in the
298 case of Willi354, with Pst seemingly following the same trend. Expression levels then rose
299 above mock-treated control by ~ 2.5-fold at 96 hpi, with changes being statistically

300 significant for 48 and 96 hpi for Pst and 96 hpi for Willi354 (Fig. **2b**). In addition, Micro347
301 showed a significant ~ 1.8-fold rise in ET marker gene expression at 96 hpi (Fig. **2b**).
302
303 Regarding the JA marker, statistically significant changes were only observed in response
304 to Sphingo34. A drop in expression was observed between 12 and 48 hpi with the latter
305 being statistically significant, but rather weak at ~ 1.5-fold (Fig. **2b**). Expression of the SA
306 marker, *PR1*, fluctuated strongly, but not significantly between up- and downregulation
307 upon Willi354 treatment. Strong fluctuations between no expression change and a strong
308 downregulation were observed following Micro347 treatment with a significant ~ 3-fold
309 decrease in expression at 24 hpi. Sphingo34 and Pst elicited no changes in *PR1* expression
310 (Fig. **2b**).
311
312 The increase in ET marker expression within the last three sampling times (24, 48, 96 hpi)
313 seemed to follow the increase in bacterial density of the inoculants (Fig. **2a, b**).
314 Interestingly, 57% (adj. R^2 = 0.57, p = 0.0027) of the change in gene expression relative to the
315 mock control can be explained by the bacterial density, irrespective of the inoculant
316 (Fig. **3**).
317

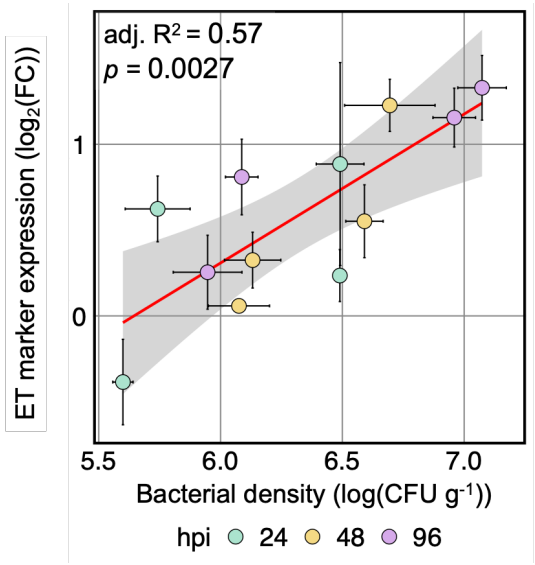

Fig. 3: Ethylene marker responses may be explained by bacterial density. Correlation between mean $\log_2$(FC) in gene expression of ethylene (ET) marker gene (*ARL2*) relative to mock-treated control and mean bacterial density. Colours depict the time of sampling post inoculation, red line depicts a fitted linear model, the grey bar depicts limits of 95% confidence interval, error bars depict standard error of the mean. n = 3 and 4 for mean $\log_2$(FC) in gene expression and mean bacterial density, respectively.

329 *Genome-wide transcriptional changes indicate strong similarity in the plant response to*
330 *various bacterial leaf colonisers*
331 The strongest changes in gene expression were observed in Pst, Willi354 and Micro347
332 treated plants at 96 hpi. To gain an understanding of genome-wide transcriptional
333 changes to individual leaf-colonising strains, the RNA of plants sampled at 96 hpi treated
334 with either Pst, Willi354 or Micro347 were further subjected to RNA sequencing. The
335 expression profiles of various target genes quantified by RNA sequencing were similar to
336 those quantified by RT-qPCR confirming that RNA sequencing was performed correctly
337 (Fig. **S2**). As expected, the transcriptomes of mock-treated plants were distinct from those
338 of inoculated plants, as shown by multi-dimensional scaling (MDS) and k-means
339 clustering (Fig. **4a**, Fig. **S3c**). The transcriptomes separate by treatment along the first
340 dimension of the MDS plot (Fig. **4a**). Mock and Pst treated samples separate the furthest,
341 corresponding to a leading FC of ~ 4-fold between the two treatments. Micro347 and
342 Willi354 treated samples cluster close to Pst with Willi354 being closer to Pst than
343 Micro347, indicating a higher overlap of differentially expressed genes (DEGs). The second
344 dimension of the MDS plot mainly separates the individual transcriptomes within a
345 treatment group, showing low variation within Micro347 samples and strong variation
346 within Willi354 samples, corresponding to a leading FC of ~ 3-fold (Fig. **4a**).
347
348 Genes with a significant FC threshold of $\log_2(1.3)$ based on the edgeR TREAT algorithm
349 (McCarthy & Smyth, 2009) and a FDR < 0.05 were defined as DEGs. This FC threshold was
350 chosen, based on the median 'elbow', the point of maximum curvature (second derivative)
351 of the number of DEGs as a function of the $\log_2$(FC) threshold per treatment (Fig. **S3a**). Pst
352 treated plants exhibited 757 DEGs at this FC threshold, followed by Willi354 with 172 DEGs
353 and Micro347 with 106 DEGs. Interestingly, almost all the DEGs in Micro347 are also
354 differentially expressed in Willi354 and Pst. In addition, almost all the DEGs found in
355 Willi354 are also differentially expressed in Pst (Fig. **4b**). This shows that plant responses
356 to these three leaf-colonising strains are largely similar but differ in their strength
357 depending on the leaf coloniser. A closer look at individual gene expression changes
358 further highlights the similarity in the responses. Most changes follow a sequence with

either increasing or decreasing expression from mock-treated control over Micro347 and Willi354 to Pst-treated plants (Fig. **4c**, Fig. **S3c**). Further, all the 770 genes that were differentially expressed in any of the treatments, were either up- or downregulated in all the treatments. No gene was significantly upregulated in one treatment and significantly downregulated in another.

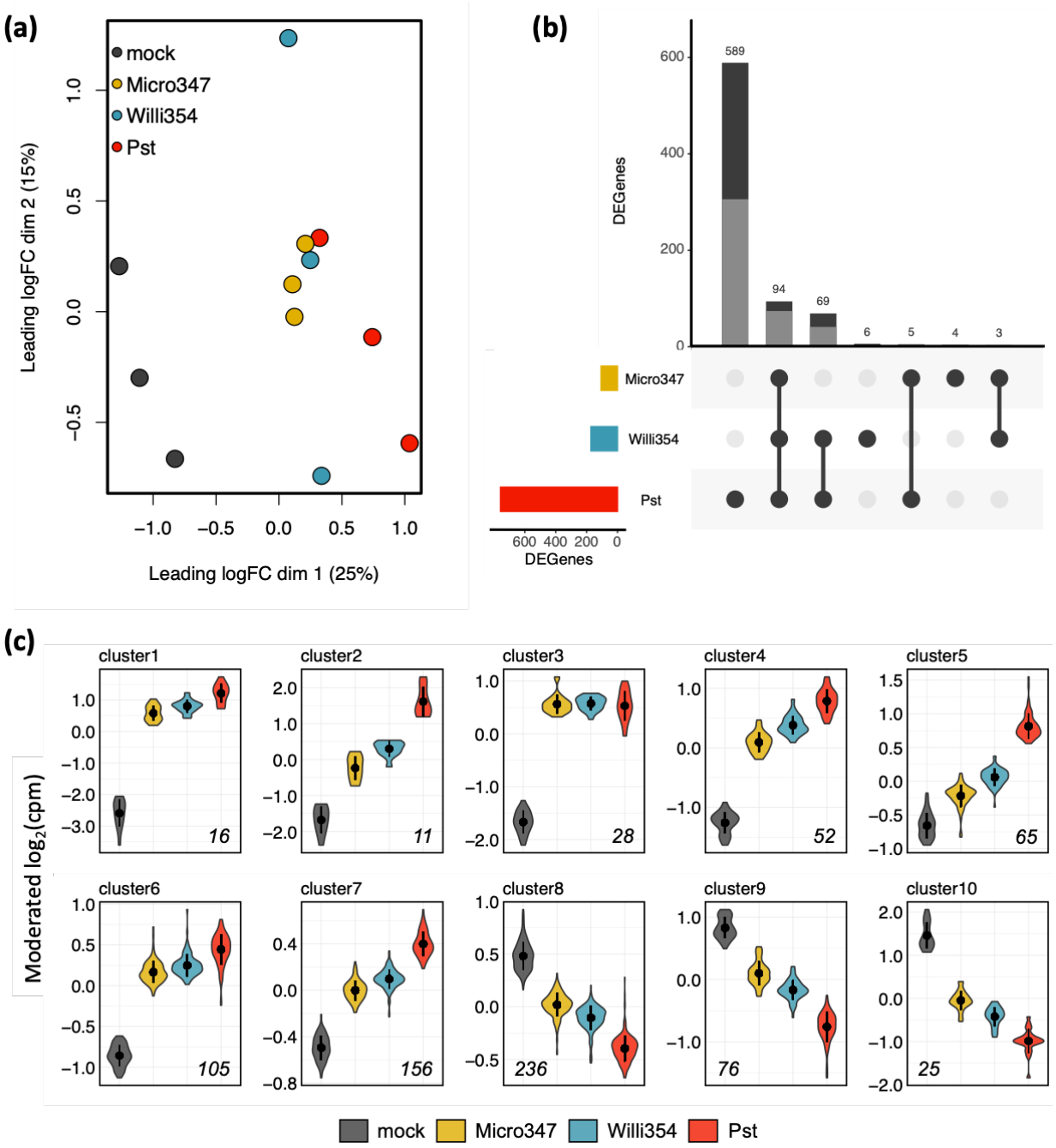

366 **Fig. 4: Comparison of transcriptomic response to various leaf-colonising strains.** (**a**)
367 Multidimensional scaling plot of transcriptomes of above ground plant parts of four-weeks-old
368 axenically-grown arabidopsis plants four days after spray-inoculation with individual bacterial
369 strains. Points depict individual transcriptomes, colour depicts inoculant or mock control treatment.
370 (**b**) UpSet plot of DEGs in the different treatments. The coloured bar chart on the left depicts the total
371 number of DEGs per treatment. The black dots in the panel's matrix depict unique (individual dots)
372 and overlapping (connected dots) DEGs. The top bar chart depicts DEGs for each unique or overlapping
373 combination in the panel's matrix. Grey bar depicts upregulated DEGs, black bar depicts
374 downregulated DEGs. (**c**) Plots showing moderated $\log_2$(cpm) of DEGs per k-means cluster of
375 transcriptomes of above ground plant parts of four-weeks-old axenically-grown arabidopsis plants
376 four days after spray-inoculation with individual bacterial strains. Colours depict the treatment, the
377 italicised number in each plot depicts the number of DEGs per cluster. Treatments were ordered based
378 on the number of DEGs. Note that the y-axis differs between different cluster-plots.
379
380 To gain a better resolution of gene expression changes, the 770 genes that were
381 differentially expressed in any of the treatments were further separated by k-means
382 clustering. K-means clustering was performed based on moderated $\log_2$(cpm). Ten k-
383 means were chosen, based on the 'elbow' of the total sum of squares as a function of the
384 number of k-means (Fig. **4c**, Fig. **S3b,c**). The 433 upregulated genes are in clusters 1-7, and
385 the 337 downregulated genes are in clusters 8-10 (Fig. **4c**, Fig. **S3c**). In addition to more
386 genes being significantly upregulated than downregulated, FCs were greater in
387 upregulated genes. Clusters 1 and 2 contain genes with the strongest upregulation and
388 cluster 10 genes with the strongest downregulation at FCs in moderated $\log_2$(cpm) of ~ 16-
389 fold and ~ 6-fold, respectively (Fig. **4c**).
390
391 *Transcriptional responses depend on bacterial load*
392 As seen above, responses to bacterial colonisation seem to be largely similar (Fig. **4b,c**) in
393 response to the tested strains. This was especially surprising as Pst is an arabidopsis
394 pathogen, whereas Micro347 and Willi354 were isolated from leaves of asymptomatic
395 plants (Cuppels, 1986; Bai *et al.*, 2015). In addition, bacterial density, irrespective of the
396 bacterial coloniser, had a highly significant effect on ethylene responses (Fig. **3**). Taken

397 together, this suggests that pathogenicity is to some extent dependent on bacterial density,
398 following Paracelcus' theory “the dose makes the poison” (Paracelsus, 1538). This raises the
399 question whether non-pathogenicity of bacteria is merely a case of the plant balancing
400 their proliferation, or the bacteria doing so in order to avoid being penalised by the plant.
401 To gain a better understanding of plant responses to non-pathogenic leaf-colonising
402 bacteria and to determine whether the bacterial load changes the nature of the response,
403 plants were inoculated with different concentrations of Willi354 followed by RNA
404 sequencing. Willi354 was chosen for this experiment as it exhibited stronger responses
405 than Micro347 in the previous experiment (Fig. **4b,c**).
406
407 Six-weeks-old axenically-grown arabidopsis plants were spray inoculated with Willi354
408 with inoculation densities ranging from 10^5 CFU ml^{-1} to 10^8 CFU ml^{-1}. Four days after
409 inoculation, the bacterial densities on the plants ranged from 6.57×10^6 CFU g^{-1} to 3.22×10^8
410 CFU g^{-1} and strongly correlated with the inoculation density (adj.R^2 = 0.9265, $p = 3.594 \times 10^{-}$
411 ^{14}) (Fig. **5a**). The transcriptomic response of the plants changed gradually with increasing
412 inoculation density, as seen in the MDS plot and k-means clustering (Fig. **5b**, Fig. **S4**). The
413 transcriptomes separate along the first dimension of the MDS plot, which explains 55% of
414 the variation between the different samples, with those of mock-treated plants and those
415 of plants inoculated with Willi354 at 10^8 CFU ml^{-1} being most dissimilar at a leading FC of ~
416 16-fold (Fig. **5b**).
417

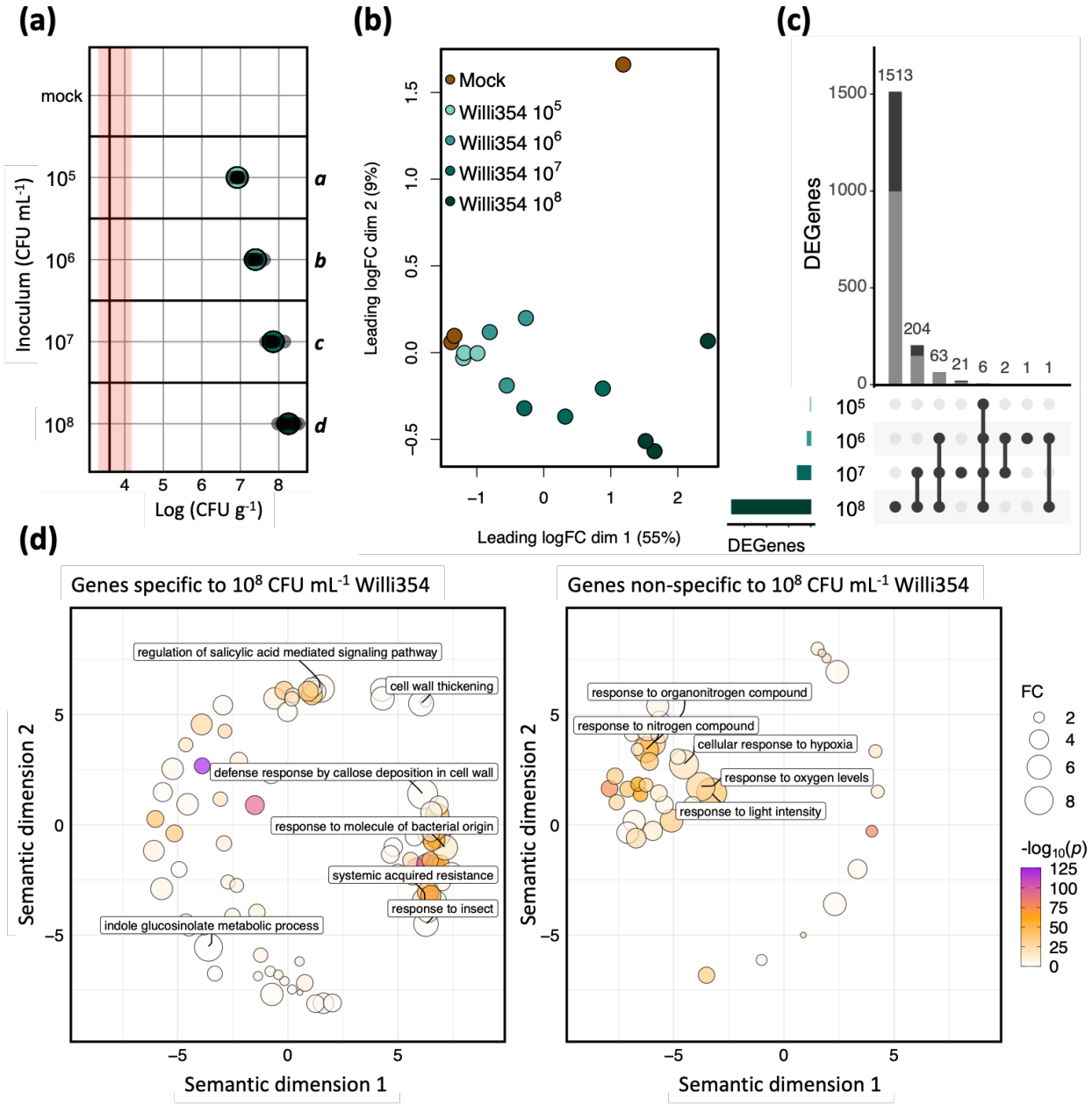

Fig. 5: Plant transcriptomic response to different densities of Willi354 (**a**) Bacterial density of Willi354 on above ground plant parts of six-weeks-old axenically-grown arabidopsis plants 96 hpi with different initial densities. Coloured circles depict the mean, bars depict standard deviation, smaller grey circles depict the bacterial density from individual biological replicates, the vertical black line represents the threshold of detection based on mean plant weight, red bar represents the threshold range of detection based on the heaviest and lightest plant. Letters on the right side of the plot depict statistical differences (p < 0.001, one-way ANOVA & Tukey's HSD test). (**b**). Multidimensional scaling plot of transcriptomes of arabidopsis above ground plant parts 96 hpi.

427 Circles depict individual transcriptomes, colour depicts inoculation density or mock control
428 treatment. (**c**) UpSet plot of transcriptomes depicted in (**b**). Genes with a FC significantly above $\log_2(1.3)$
429 and a FDR < 0.05 were defined as DEGs. In each panel, the bottom left bar chart depicts the overall
430 number of DEGs per treatment. The dots in the panel's matrix depict unique (individual dots) and
431 overlapping (connected dots) DEGs. The top bar chart depicts DEGs for each unique or overlapping
432 combination in the panel's matrix. Grey bar depicts upregulated DEGs, black bar depicts
433 downregulated DEGs. (**d**) Functional enrichment of genes specifically and non-specifically expressed
434 to high densities of Willi354. Functional enrichment of GO terms distributed in the semantic space.
435 Closeness in semantic space ideally reflects closeness in GO term structure. Circles depicted
436 significantly enriched GO terms ($p < 0.05$, Bonferroni corrected). Circle size depicts fold enrichment,
437 colour depicts $-\log_{10}(p)$. GO terms with a FC > 6 are labelled.
438
439 Genes were defined as DEGs as described above. Plants treated with 10^5, 10^6, 10^7 and 10^8 CFU
440 ml^{-1} of Willi354 exhibited 6, 73, 296 and 1787 DEGs, respectively. A total of 1811 genes were
441 differentially expressed across all treatments, with ~ 68% (1230 DEGs) being upregulated
442 (Fig. **5c**). Further, upregulated genes exhibited stronger changes in gene expression, the
443 strongest being ~ 30-fold in moderated $\log_2$(cpm), compared to downregulated genes, the
444 strongest being ~ 4-fold in moderated $\log_2$(cpm) (Fig. **S5**). This highlights that positive
445 expression changes are not only more prominent, but also stronger than negative
446 expression changes. The DEGs were separated by k-means clustering into 10 clusters.
447 Clusters 1-8 contained the upregulated, and clusters 9 and 10 contained the downregulated
448 genes (Fig. **S4c**, Fig. **S5**). Most genes showed no marked difference between mock-treated
449 plants and plants treated with Willi354 at 10^5 and 10^6 CFU ml^{-1}. At concentrations of 10^7 and
450 10^8 CFU ml^{-1}, genes in clusters 1, 3, 4,6 and 8 were strongly upregulated, with genes at 10^8
451 being upregulated twice as much compared to those at 10^7 (Fig. **S5**). Genes in clusters 5 and
452 7 appear to follow a sigmoidal curve, with no difference in gene expression between plants
453 inoculated with Willi354 at 10^7 and 10^8 CFU ml^{-1} in cluster 7 (Fig. **S5**). Genes in clusters 9
454 and 10 exponentially decreased in expression with increasing density of Willi354 (Fig. **S5**).
455
456 To further explore the nature of plant responses to inoculation with Willi354, a GO term
457 enrichment analysis was performed on two different sets of genes. The first set comprised

458 genes that were exclusively differentially expressed in plants treated with Willi354 at
459 10^8 CFU ml^{-1}, whereas the second set comprised genes that were also differentially
460 expressed at lower densities of Willi354. The functional profiles of both sets of genes were
461 markedly different (Fig. **5d**). Genes differentially expressed exclusively at the highest
462 density of Willi354, were greatly enriched for genes related to plant immunity, including
463 perception of the biotic environment, such as 'response to molecule of bacterial origin' and
464 'response to insect', metabolism of secondary metabolites such as 'indole glucosinolate
465 metabolic process', local defence responses such as 'cell wall thickening' and 'defence
466 response by callose deposition in cell wall', and systemic defence responses such as
467 'regulation of salicylic acid mediated signalling pathway' and 'systemic acquired
468 resistance' (Fig. **5d**). By contrast, genes that were also differentially expressed at lower
469 densities of Willi354, were greatly enriched for genes related to plant nitrogen
470 homeostasis, such as 'response to nitrogen compound' and 'response to organonitrogen
471 compound', plant oxygen levels, such as 'response to oxygen levels' and 'response to
472 hypoxia' and the plant's 'response to light intensity' (Fig. **5d**).
473

474 *Transcriptional changes induced by bacteria may depend on the chromatin state of a*
475 *given gene*

476 A major determinant of gene transcriptional regulation is the chromatin state of genes.
477 Chromatin states are determined by the combination of chromatin modifications and
478 histone variants. Various histone modifications, such as H3K4me3, H3K36me3 and lysine
479 acetylation, were previously shown to contribute to the induction of genes in response to
480 pathogen exposure (Berr *et al.*, 2012; Ding & Wang, 2015). As genes specifically induced by
481 high densities of Willi354 presented distinct functional enrichment than genes induced by
482 Willi354 irrespective of inoculation density, we hypothesised that both of sets of genes,
483 genes activated after high inoculation and genes activated irrespectively of inoculation
484 density, might exhibit different chromatin states prior to inoculation. To that end, the state
485 of both sets of genes was examined using the chromatin state topology established by
486 Sequeira-Mendes et al. (2014) (Fig. **6a**). Both sets exhibited an enrichment of states 1 and 2,
487 which are both characterised by the presence of the histone variant H2A.Z accompanied

488 either by activating marks such as H3K4me3, H3K36me3 or by a combination of activating
489 (H3K4me3) and repressive (H3K27me3) marks, respectively. They also displayed an
490 underrepresentation of states 8 and 9, which contain heterochromatic marks such as
491 H3K9me2 and H3K27me1. In addition, genes which are upregulated by Willi354
492 irrespective of inoculation density showed an underrepresentation of states 3, 5, 6 and 7.
493 By contrast, genes solely induced by the highest density of Willi354 either showed an
494 enrichment (state 6) or no difference to the reference. These results reveal that, similarly to
495 the distinct functional enrichments, genes induced specifically by higher bacterial
496 densities exhibit a partially different chromatin signature than genes that are also induced
497 by lower densities.
498
499 As the genes induced solely by the higher densities of Willi354 displayed an enrichment
500 for plant immunity and defence-related terms (Fig. **5d**), we wondered whether those genes
501 would have a similar chromatin profile as genes induced by Pst. The genes were divided
502 into two sets, depending on whether they were induced specifically by Pst or whether they
503 were also induced by Willi354 or Micro347 (Fig. **6b**). Similarly, to the previous analysis,
504 both sets presented an enrichment for states 1 and 2 and an underrepresentation for states
505 8 and 9. They also showed an underrepresentation of state 5, characterised by the presence
506 of the repressive mark H3K27me3. Additionally, genes induced by both Pst or
507 Willi354/Micro347 displayed an underrepresentation of states 6 and 7, which was not
508 observed or of reduced magnitude for the genes induced specifically by Pst. Despite limited
509 overlap between the two transcriptomic experiments (Fig. **S6**), the chromatin profiles of
510 genes induced specifically either by high Willi354 densities or Pst were comparable and
511 distinct from the profiles of genes induced also by non-pathogenic bacteria or by lower
512 bacterial densities. This observation supports the idea that inoculation with higher
513 densities of non-pathogenic bacteria leads to a transcriptomic response similar to that
514 triggered by pathogenic bacteria.

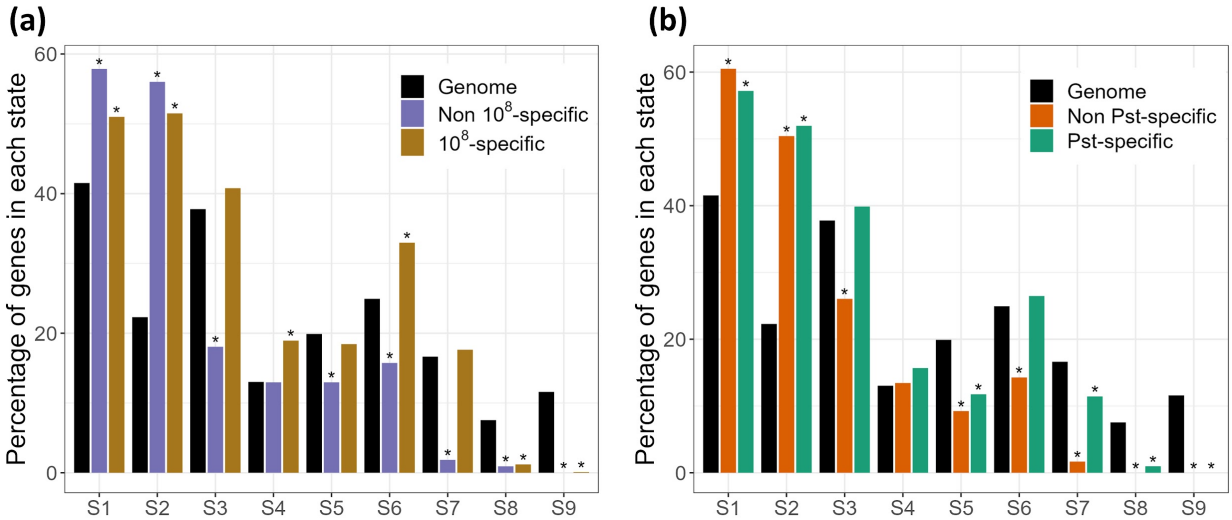

Fig. 6: Chromatin state analysis of genes upregulated following bacterial inoculation. (**a**). Chromatin state analysis of genes induced either specifically by the highest density (10^8) of Willi354 or also induced by lower inoculant densities (10^5, 10^6 or 10^7). (**b**) Chromatin state analysis of genes induced either specifically by Pst or also induced by Willi354 or Micro347 (all at a density of 10^7). The chromatin states coordinates were obtained from Sequeira-Mendes et al. (2014). * indicates significant difference compared to the genome, tested by Marascuilo procedure (α = 0.05).

High densities of Willi354 caused slight disease phenotypes

Since the genes that were uniquely differentially expressed in plants inoculated with Willi354 at 10^8 CFU ml^{-1} were enriched for plant immunity-related genes, plants were inoculated with Willi354 under the previous experimental conditions and sampled at 14 and 21 dpi, to investigate if Willi354 evokes plant disease phenotypes. Indeed, plants inoculated with Willi354 at 10^8 CFU ml^{-1}, but not at lower densities, exhibited necrotic lesions on a few leaves 14 and 21 dpi (Fig .**7a-f**, Fig. **S7**). In addition, plant weight was negatively correlated with inoculation density of Willi354 (adj.R^2 = 0.11, $p = 6.48 \times 10^{-5}$) (Fig. **7h**).

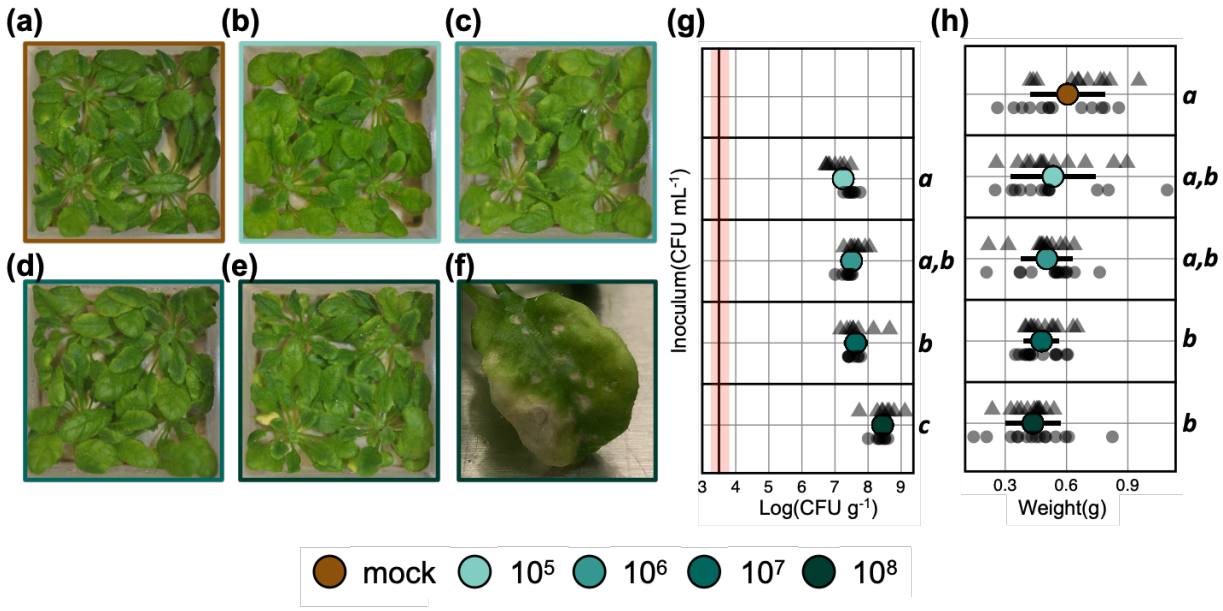

Fig. 7: Effect of Willi354 density on plant phenotype 21 dpi. Representative images of six-weeks-old axenically-grown arabidopsis plants. Plants were either mock-treated (**a**) or inoculated with Willi354 at 10^5 CFU ml^{-1} (**b**), 10^6 CFU ml^{-1} (**c**), 10^7 CFU ml^{-1} (**d**) or 10^8 CFU ml^{-1} (**e**). (**f**) Representative image of the leaves that showed spots of localised cell death in plants inoculated with Willi354 at 10^8 CFU ml^{-1}. (**g**) Bacterial density of Willi354 on aboveground plant parts of six-weeks-old axenically-grown arabidopsis plants. The vertical black line represents the threshold of detection based on mean plant weight, the red bar represents the threshold range of detection based on the heaviest and lightest plant. (**h)** Fresh weight of six-weeks-old axenically-grown arabidopsis plants. Coloured circles depict the mean, bars depict standard deviation, smaller grey shapes depict the bacterial density from individual biological replicates of two independent experiments. Letters on the right side of the plots depict statistical differences ($p < 0.05$), one-way ANOVA & Tukey's HSD test.

545 ## Discussion

546

547 *Temporal responses of the plant immune system*

548 Bacteria were spray-inoculated at densities that matched the bacterial carrying capacity of
549 leaves in temperate environments (Kniskern *et al.*, 2007; Reisberg *et al.*, 2012; Rastogi *et al.*,
550 2012; Burch *et al.*, 2016; Gekenidis *et al.*, 2017). Four of the six inoculated bacteria
551 successfully established on plant leaves, whereas two, Acido84 and Pedo194, failed to
552 consistently reach bacterial densities above the threshold of detection, which was on
553 average ~ 2500 CFU g^{-1} of leaf fresh weight (Fig. **2a**). This was rather surprising as both
554 genera were previously found to make up more than 1% of the total bacterial population on
555 arabidopsis (Vorholt, 2012). Further, both strains were recently shown to successfully
556 colonise arabidopsis (Vogel *et al.*, 2021). However, in the study by Vogel and colleagues,
557 colonisation density was measured nine days after drop inoculation on seedlings in an
558 agar-based system. In this study the 'Litterbox' system was employed, which reliably
559 mimics environmental population densities, as opposed to agar-based systems that exhibit
560 unnaturally high population densities (Miebach *et al.*, 2020). In addition, Acido84 reached
561 population densities of 10^4 - 10^6 CFU g^{-1} in all sampled plants at 168 hpi (i.e. 7 dpi). Since
562 Acido84 was also successfully recovered straight after inoculation this indicates (1) that
563 Acido84 was not harmed during the spraying procedure and (2) that it was able to thrive
564 on leaves at later time points. Overall, this suggests that Acido84 had to acclimatise to its
565 new environment after growth on R2A media, even though R2A is, like the phyllosphere,
566 oligotrophic. Pedo194, in contrast, was only successfully recovered from one plant
567 immediately after spray-inoculation at a density ~ 2 magnitudes lower than the inoculum,
568 suggesting that the inoculation procedure might have been detrimental to it.

569

570 Pst and Will354 rose in population size to ~ 10^7 CFU g^{-1} at 96 hpi. Population size then
571 declined to 10^6 CFU g^{-1} at 168 hpi (Fig. **2a**). Whether this was due to exhaustion of resources
572 or plant immune responses remains to be determined. Interestingly though, the expression
573 of the ET marker *ARL2* could be explained in large parts by the bacterial density of the
574 coloniser, irrespective of the inoculant. This suggests that *ARL2* expression must be either

575 triggered by a common MAMP, shared between the isolates, or was triggered by many
576 MAMPs which the plant did not distinguish between. Further, it suggests that *ARL2*
577 expression is proportional to the MAMP titer. This agrees with previous findings, which
578 described stronger transcriptional responses to both higher pathogen and higher MAMP
579 titers (Thilmony *et al.*, 2006; Denoux *et al.*, 2008).
580
581 The observed expression changes upon bacterial treatment were overall rather weak (Fig.
582 **2b**). The strongest changes in gene expression were observed in the ET marker, *ARL2*, and
583 culminated at 96 hpi. As expected, the strongest changes were observed in the plants
584 treated with Pst. The overall weak and rather late response seemingly disagrees with
585 previous studies describing fast and substantial changes in gene expression upon MAMP
586 treatment and infection with Pst (Thilmony *et al.*, 2006; Zipfel *et al.*, 2006; Denoux *et al.*,
587 2008; Bjornson *et al.*, 2021). However, in these studies either young seedlings were treated
588 by a complete change of media, with the fresh media containing the MAMP or leaves of
589 mature plants were vacuum infiltrated. In both cases MAMPs were readily available. By
590 contrast, in the case of a surface spray, a sufficient amount of eliciting molecules needs to
591 cross the hydrophobic cuticle layer to reach the plasma membranes of plant cells
592 (Schlechter *et al.*, 2019) or bacteria need to migrate into the apoplast (Beattie & Lindow,
593 1999; Melotto *et al.*, 2006). In addition, the flg22 receptor, FLS2 is highly expressed in leaves
594 near bacterial entry sites, such as stomata, which are predominantly found on the abaxial
595 (lower) leaf surface and hydathodes, as well as in leaf veins (Beck *et al.*, 2014). Vacuum
596 infiltration of bacterial suspensions would render leaf veins more exposed to MAMPs and
597 a change in liquid media would render stomata and hydathodes more exposed to MAMPs,
598 than in the more 'natural' scenario of topical application.

599 *Genome-wide transcriptional responses to leaf colonisation*

600

601 *Plant responses to non-pathogenic bacteria are qualitatively similar but differ*
602 *quantitatively compared to pathogenic bacteria*

603 Bacterial colonisation with non-pathogenic leaf colonisers significantly altered the
604 expression of several genes in the host, although not to the extent of a pathogenic leaf
605 coloniser. Remarkably, the responses observed were largely similar, but weaker in
606 response to colonisation by the non-pathogenic bacteria. Most genes significantly
607 expressed in response to one strain were also significantly expressed in response to
608 strains that elicited stronger responses and thus, higher numbers of DEGs. None of the 770
609 genes with a significant FC in any of the bacterial treatments was upregulated by one
610 strain and downregulated by another. Changes in gene expression of genes belonging to
611 clusters 2, 4, 5, 6, 7, 8, 9 and 10 were either progressively increasing or decreasing when
612 treatments were sorted by the number of DEGs that they elicited (Fig. **4c**). This indicates
613 that those genes were similarly regulated in response to bacterial colonisation irrespective
614 of the symbiotic relationship of the inoculant with the plant, although less severely in
615 response to non-pathogenic bacteria. Such similarity in the plant response to various leaf
616 colonisers was also described recently by Maier and colleagues, although without the
617 context of a pathogenic bacterium (Maier *et al.*, 2021). Interestingly, the response strength
618 was strongly driven by the bacterial density of the inoculant (Maier *et al.*, 2021), which was
619 also observed in the current study with respect to ET marker responses to non-pathogenic
620 and pathogenic bacteria. This suggests that plants merely responded to a pool of bacterial
621 MAMPs quantitatively, by responding to the total amount of MAMPs present, rather than
622 qualitatively by integrating a unique mix of different MAMPs into a tailored plant
623 response.

624

625 *The effect of bacterial load on plant gene expression*

626 Bacterial densities were the major driver of ethylene marker expression between 24 and 96
627 hpi irrespective of the bacterial coloniser (Fig. **3**). In addition, genome-wide transcriptional
628 responses to bacterial colonisation were largely similar but differed in number of DEGs

629 (Fig. **4b**), as well as in the expression strength of individual genes (Fig. **4c**). This was
630 remarkable, as the tested strains included bacteria isolated from asymptomatic plants (Bai
631 *et al.*, 2015) as well as pathogenic Pst (Cuppels, 1986). As pathogenicity is linked to bacterial
632 density, this raises the question whether non-pathogenicity is merely a case of the plant
633 limiting uncontrolled proliferation via Pattern Triggered Immunity or bacteria limiting
634 their proliferation to avoid being penalised by the plant.
635
636 Plants were inoculated with Willi354 at various concentrations, resulting in different
637 bacterial densities ranging from somewhat natural densities ~ 10^6 - 10^7 CFU g^{-1} to
638 artificially high densities ~ 10^8 - 10^9 CFU g^{-1} within 96 hpi (Fig. **5a**). These differences in
639 bacterial densities were still observed at 21 dpi (Fig. **7g**). The maximal bacterial load,
640 referred to as the carrying capacity, strongly correlated with the inoculation density (Fig.
641 **5a**), as was previously demonstrated on bean leaves (Wilson & Lindow, 1994; Remus-
642 Emsermann *et al.*, 2012). Interestingly, severe disease phenotypes were observed on a few
643 leaves of plants colonised by Willi354 at ~ 10^8 - 10^9 CFU g^{-1} 14 and 21 dpi (Fig. **7e,f**, Fig. **S7**). In
644 addition, plant weight negatively correlated with bacterial density (Fig. **7g,h**). This
645 suggests that bacteria that are otherwise non-pathogenic can be detrimental to the plant at
646 very high densities.
647
648 RNA sequencing revealed an exponential increase in both the number of DEGs and the
649 expression pattern of most DEGs to increasing bacterial densities (Fig. **5c**, Fig. **S5**). In
650 addition, gene expression changes were relatively strong in upregulated genes with FCs up
651 to ~ 30-fold (Fig. **S5**). This suggests that the plant barely invests energy into an interaction
652 with its bacterial colonisers at low bacterial densities, but drastically increases responses
653 when bacteria are reaching potentially dangerous levels. Accordingly, genes that were
654 uniquely differentially expressed in plants harbouring Willi354 at ~ 10^8 - 10^9 CFU g^{-1} were
655 greatly enriched for immune related GO terms, including perception of the biotic
656 environment ('response to molecule of bacterial origin', 'response to insect'), metabolism of
657 secondary metabolites ('indole glucosinolate metabolic process'), local defence responses
658 ('cell wall thickening', 'defence response by callose deposition in cell wall'), and systemic

defence responses ('regulation of salicylic acid mediated signalling pathway', 'systemic acquired resistance') (Fig. **7d**).

Because the plant 'ignores' bacteria at low densities, it appears unlikely that the plant limits bacterial proliferation by active signalling processes at low bacterial densities. Consequently, it is likely that bacteria limit their proliferation in order not to alert the plant immune system. This is in agreement with recent findings showing endophytic bacteria remaining in population stasis by a multiplication-death equilibrium independent of bacterial density (Velásquez *et al.*, 2022).

The chromatin state analysis further supported the idea that artificially high densities of non-pathogenic bacteria lead to a transcriptomic response similar to that triggered by pathogenic bacteria. Genes induced by bacterial inoculation, both at pathogenic and non-pathogenic level, were enriched for the chromatin states 1 and 2 (Fig. **6**). In more detail they were enriched in H2A.Z and H3K4me3-H3K27me3 marks, previously shown to be essential for gene responsiveness to environmental changes (Coleman-Derr & Zilberman, 2012; Sura *et al.*, 2017; Faivre & Schubert, 2023).This suggests that these chromatin marks might be guiding the transcriptomic response of the plant to bacterial inoculation.

Conclusion

We show that plant responses to various leaf colonising bacteria are largely similar, both in the overlap of DEGs and the expression of individual DEGs but differ in expression strength. We tested the competing hypotheses that plants are either 1) monitoring bacterial population density or 2) differentiating between different bacterial colonisers. Our results suggest that plants are responding to bacterial densities rather than bacterial identities, favouring hypothesis 1) to be the more prevalent mode of plant response to bacteria. It appears that the plant barely invests resources into an interaction with its associated bacteria at low bacterial densities, but markedly increases gene expression towards defence responses upon high bacterial colonisation.

Acknowledgements

This work was supported by Marsden Fast Start grant number 17-UOC-057 to M.N.P.R.-E. by the Royal Society Te Apārangi. M.M. was supported by a University of Canterbury Ph.D. scholarship.

Author contributions

M.M., P.E.J. and M.N.P.R.-E. conceived and designed the study. M.M. performed all laboratory experiments and analysed the data. L.F. and D.S performed additional data analysis. M.M. wrote the initial draft of the manuscript and all authors contributed to later versions of the manuscript and to data interpretation.

Conflict of interest

The authors declare that they have no conflict of interest

701 ## References

702 Bai Y, Müller DB, Srinivas G, Garrido-Oter R, Potthoff E, Rott M, Dombrowski N, Münch PC,
703 Spaepen S, Remus-Emsermann M, *et al.* 2015. Functional overlap of the Arabidopsis leaf
704 and root microbiota. *Nature* 528: 364–369.

705 Beattie GA, Lindow SE. 1999. Bacterial colonization of leaves: A spectrum of strategies.
706 *Phytopathology®* 89: 353–359.

707 Beck M, Wyrsch I, Strutt J, Wimalasekera R, Webb A, Boller T, Robatzek S. 2014. Expression
708 patterns of flagellin sensing 2 map to bacterial entry sites in plant shoots and roots.
709 *Journal of experimental botany* 65: 6487–6498.

710 Berr A, Ménard R, Heitz T, Shen W-H. 2012. Chromatin modification and remodelling: a
711 regulatory landscape for the control of Arabidopsis defence responses upon pathogen
712 attack. *Cellular microbiology* 14: 829–839.

713 Bjornson M, Pimprikar P, Nürnberger T, Zipfel C. 2021. The transcriptional landscape of
714 *Arabidopsis thaliana* pattern-triggered immunity. *Nature plants* 7: 579–586.

715 Burch AY, Do PT, Sbodio A, Suslow TV, Lindow SE. 2016. High-level culturability of
716 epiphytic bacteria and frequency of biosurfactant producers on leaves. *Applied and*
717 *environmental microbiology* 82: 5997–6009.

718 Chen L-Q, Hou B-H, Lalonde S, Takanaga H, Hartung ML, Qu X-Q, Guo W-J, Kim J-G,
719 Underwood W, Chaudhuri B, *et al.* 2010. Sugar transporters for intercellular exchange and
720 nutrition of pathogens. *Nature* 468: 527–532.

721 Coleman-Derr D, Zilberman D. 2012. Deposition of histone variant H2A.Z within gene bodies
722 regulates responsive genes. *PLoS genetics* 8: e1002988.

723 Cuppels DA. 1986. Generation and characterization of Tn5 insertion mutations in
724 *Pseudomonas syringae* pv. tomato. *Applied and environmental microbiology* 51: 323–327.

725 Czechowski T, Stitt M, Altmann T, Udvardi MK, Scheible W-R. 2005. Genome-wide

726 identification and testing of superior reference genes for transcript normalization in
727 Arabidopsis. *Plant physiology* **139**: 5–17.

728 **Denoux C, Galletti R, Mammarella N, Gopalan S, Werck D, De Lorenzo G, Ferrari S, Ausubel**
729 **FM, Dewdney J. 2008**. Activation of defense response pathways by OGs and Flg22 elicitors
730 in Arabidopsis seedlings. *Molecular plant* **1**: 423–445.

731 **Ding B, Wang G-L. 2015**. Chromatin versus pathogens: the function of epigenetics in plant
732 immunity. *Frontiers in plant science* **6**: 675.

733 **Dombrecht B, Xue GP, Sprague SJ, Kirkegaard JA, Ross JJ, Reid JB, Fitt GP, Sewelam N,**
734 **Schenk PM, Manners JM, *et al.* 2007**. MYC2 differentially modulates diverse jasmonate-
735 dependent functions in Arabidopsis. *The Plant cell* **19**: 2225–2245.

736 **Durinck S, Moreau Y, Kasprzyk A, Davis S, De Moor B, Brazma A, Huber W. 2005**. BioMart
737 and Bioconductor: a powerful link between biological databases and microarray data
738 analysis. *Bioinformatics* **21**: 3439–3440.

739 **Faivre L, Schubert D. 2023**. Facilitating transcriptional transitions: an overview of
740 chromatin bivalency in plants. *Journal of experimental botany* **74**: 1770–1783.

741 **Gekenidis M-T, Gossin D, Schmelcher M, Schöner U, Remus-Emsermann MNP, Drissner D.**
742 **2017**. Dynamics of culturable mesophilic bacterial communities of three fresh herbs and
743 their production environment. *Journal of applied microbiology* **123**: 916–932.

744 **Hacquard S, Garrido-Oter R, González A, Spaepen S, Ackermann G, Lebeis S, McHardy AC,**
745 **Dangl JL, Knight R, Ley R, *et al.* 2015**. Microbiota and host nutrition across plant and animal
746 kingdoms. *Cell host & microbe* **17**: 603–616.

747 **He Z, Webster S, He SY. 2022**. Growth–defense trade-offs in plants. *Current biology: CB* **32**:
748 R634–R639.

749 **Huot B, Yao J, Montgomery BL, He SY. 2014**. Growth-defense tradeoffs in plants: a
750 balancing act to optimize fitness. *Molecular plant* **7**: 1267–1287.

751 Innerebner G, Knief C, Vorholt JA. 2011. Protection of *Arabidobsis thaliana* against leaf-
752 pathogenic *Pseudomonas syringae* by Sphingomonas strains in a controlled model
753 system. *Applied and environmental microbiology* 77: 3202–3210.

754 Ji P, Wilson M. 2002. Assessment of the importance of similarity in carbon source
755 utilization profiles between the biological control agent and the pathogen in biological
756 control of bacterial speck of tomato. *Applied and environmental microbiology* 68: 4383–
757 4389.

758 Kelly S, Mun T, Stougaard J, Ben C, Andersen SU. 2018. Distinct *Lotus japonicus*
759 transcriptomic responses to a spectrum of bacteria ranging from symbiotic to pathogenic.
760 *Frontiers in plant science* 9: 1218.

761 Kim Y, Tsuda K, Igarashi D, Hillmer RA, Sakakibara H, Myers CL, Katagiri F. 2014.
762 Mechanisms underlying robustness and tunability in a plant immune signaling network.
763 *Cell host & microbe* 15: 84–94.

764 Kniskern JM, Traw MB, Bergelson J. 2007. Salicylic acid and jasmonic acid signaling
765 defense pathways reduce natural bacterial diversity on *Arabidopsis thaliana*. *Molecular*
766 *plant-microbe interactions: MPMI* 20: 1512–1522.

767 La Camera S, L'Haridon F, Astier J, Zander M, Abou-Mansour E, Page G, Thurow C,
768 Wendehenne D, Gatz C, Métraux J-P, *et al.* 2011. The glutaredoxin ATGRXS13 is required to
769 facilitate *Botrytis cinerea* infection of *Arabidopsis thaliana* plants: Role of ATGRXS13
770 during *B. cinerea* infection. *The Plant journal: for cell and molecular biology* 68: 507–519.

771 Lau JA, Lennon JT. 2012. Rapid responses of soil microorganisms improve plant fitness in
772 novel environments. *Proceedings of the National Academy of Sciences of the United*
773 *States of America* 109: 14058–14062.

774 Liao Y, Smyth GK, Shi W. 2014. featureCounts: an efficient general-purpose read
775 summarization program. *Bioinformatics* 30: 923–930.

776 Maier BA, Kiefer P, Field CM, Hemmerle L, Bortfeld-Miller M, Emmenegger B, Schäfer M,
777 Pfeilmeier S, Sunagawa S, Vogel CM, *et al.* 2021. A general non-self response as part of
778 plant immunity. *Nature plants* 7: 696–705.

779 Martin M. 2011. Cutadapt removes adapter sequences from high-throughput sequencing
780 reads. *EMBnet.journal* 17: 10–12.

781 McCarthy DJ, Chen Y, Smyth GK. 2012. Differential expression analysis of multifactor RNA-
782 Seq experiments with respect to biological variation. *Nucleic acids research* 40: 4288–4297.

783 McCarthy DJ, Smyth GK. 2009. Testing significance relative to a fold-change threshold is a
784 TREAT. *Bioinformatics* 25: 765–771.

785 Melotto M, Underwood W, Koczan J, Nomura K, He SY. 2006. Plant stomata function in
786 innate immunity against bacterial invasion. *Cell* 126: 969–980.

787 Miebach M, Schlechter RO, Clemens J, Jameson PE, Remus-Emsermann MNP. 2020.
788 Litterbox-a gnotobiotic zeolite-clay system to investigate arabidopsis-microbe
789 interactions. *Microorganisms* 8.

790 Mi H, Ebert D, Muruganujan A, Mills C, Albou L-P, Mushayamaha T, Thomas PD. 2021.
791 PANTHER version 16: a revised family classification, tree-based classification tool,
792 enhancer regions and extensive API. *Nucleic acids research* 49: D394–D403.

793 Moore JW, Loake GJ, Spoel SH. 2011. Transcription dynamics in plant immunity. *The Plant*
794 *cell* 23: 2809–2820.

795 Nolan T, Huggett JF, Sanchez E. 2013. Good practice guide for the application of
796 quantitative PCR (qPCR). *LGC*.

797 Paracelsus. 1538. Die dritte Defension wegen des Schreibens der neuen Rezepte. In:
798 Paracelsus, ed. Septem Defensiones: Die Selbstverteidigung eines Aussenseiters.

799 Pieterse CM, van Wees SC, Hoffland E, van Pelt JA, van Loon LC. 1996. Systemic resistance
800 in Arabidopsis induced by biocontrol bacteria is independent of salicylic acid
801 accumulation and pathogenesis-related gene expression. *The Plant cell* 8: 1225–1237.

802 Rastogi G, Sbodio A, Tech JJ, Suslow TV, Coaker GL, Leveau JHJ. 2012. Leaf microbiota in
803 an agroecosystem: spatiotemporal variation in bacterial community composition on field-
804 grown lettuce. *The ISME journal* 6: 1812–1822.

805 Reisberg EE, Hildebrandt U, Riederer M, Hentschel U. 2012. Phyllosphere bacterial
806 communities of trichome-bearing and trichomeless *Arabidopsis thaliana* leaves. *Antonie*
807 *van Leeuwenhoek* 101: 551–560.

808 Remus-Emsermann MNP, Tecon R, Kowalchuk GA, Leveau JHJ. 2012. Variation in local
809 carrying capacity and the individual fate of bacterial colonizers in the phyllosphere. *The*
810 *ISME journal* 6: 756–765.

811 Ritpitakphong U, Falquet L, Vimoltust A, Berger A, Métraux J-P, L'Haridon F. 2016. The
812 microbiome of the leaf surface of Arabidopsis protects against a fungal pathogen. *The New*
813 *phytologist* 210: 1033–1043.

814 Robinson MD, McCarthy DJ, Smyth GK. 2010. edgeR: a Bioconductor package for differential
815 expression analysis of digital gene expression data. *Bioinformatics* 26: 139–140.

816 Robinson MD, Oshlack A. 2010. A scaling normalization method for differential expression
817 analysis of RNA-seq data. *Genome biology* 11: R25.

818 Schlechter RO, Miebach M, Remus-Emsermann MNP. 2019. Driving factors of epiphytic
819 bacterial communities: A review. *Journal of advertising research* 19: 57–65.

820 Sequeira-Mendes J, Aragüez I, Peiró R, Mendez-Giraldez R, Zhang X, Jacobsen SE, Bastolla
821 U, Gutierrez C. 2014. The functional topography of the Arabidopsis genome is organized in
822 a reduced number of linear motifs of chromatin states. *The Plant cell* 26: 2351–2366.

823 Singh SK, Wu X, Shao C, Zhang H. 2022. Microbial enhancement of plant nutrient
824 acquisition. *Stress Biology* 2: 3.

825 Spaepen S, Vanderleyden J, Okon Y. 2009. Chapter 7 plant growth-promoting actions of
826 Rhizobacteria. In: Adv. Bot. Res. Academic Press, 283–320.

827 Sura W, Kabza M, Karlowski WM, Bieluszewski T, Kus-Slowinska M, Pawełoszek Ł,
828 Sadowski J, Ziolkowski PA. 2017. Dual role of the histone variant H2A.Z in transcriptional
829 regulation of stress-response genes. *The Plant cell* 29: 791–807.

830 Thilmony R, Underwood W, He SY. 2006. Genome-wide transcriptional analysis of the
831 *Arabidopsis thaliana* interaction with the plant pathogen *Pseudomonas syringae* pv.
832 *tomato* DC3000 and the human pathogen *Escherichia coli* O157:H7. *The Plant journal: for*
833 *cell and molecular biology*.

834 Velásquez AC, Huguet-Tapia JC, He SY. 2022. Shared in planta population and
835 transcriptomic features of nonpathogenic members of endophytic phyllosphere
836 microbiota. *Proceedings of the National Academy of Sciences of the United States of*
837 *America* 119: e2114460119.

838 Vogel C, Bodenhausen N, Gruissem W, Vorholt JA. 2016. The Arabidopsis leaf
839 transcriptome reveals distinct but also overlapping responses to colonization by
840 phyllosphere commensals and pathogen infection with impact on plant health. *The New*
841 *phytologist* 212: 192–207.

842 Vogel CM, Potthoff DB, Schäfer M, Barandun N, Vorholt JA. 2021. Protective role of the
843 Arabidopsis leaf microbiota against a bacterial pathogen. *Nature microbiology* 6: 1537–
844 1548.

845 Vorholt JA. 2012. Microbial life in the phyllosphere. *Nature reviews. Microbiology* 10: 828–
846 840.

847 **Wang Q, Liu J, Zhu H. 2018**. Genetic and molecular mechanisms underlying symbiotic
848 specificity in Legume-*Rhizobium* interactions. *Frontiers in plant science* **9**: 313.

849 **Wilson M, Lindow SE. 1994**. Inoculum density-dependent mortality and colonization of the
850 phyllosphere by *Pseudomonas syringae*. *Applied and environmental microbiology* **60**:
851 2232–2237.

852 **Yamada K, Saijo Y, Nakagami H, Takano Y. 2016**. Regulation of sugar transporter activity
853 for antibacterial defense in Arabidopsis. *Science* **354**: 1427–1430.

854 **Zengerer V, Schmid M, Bieri M, Müller DC, Remus-Emsermann MNP, Ahrens CH, Pelludat**
855 **C. 2018**. *Pseudomonas orientalis* F9: a potent antagonist against phytopathogens with
856 phytotoxic effect in the apple flower. *Frontiers in microbiology* **9**: 145.

857 **Zipfel C, Kunze G, Chinchilla D, Caniard A, Jones JDG, Boller T, Felix G. 2006**. Perception of
858 the bacterial PAMP EF-Tu by the receptor EFR restricts Agrobacterium-mediated
859 transformation. *Cell* **125**: 749–760.